

SUPPLEMENTAL MATERIAL

Döring et al. – Vascular CXCR4 limits atherosclerosis by maintaining arterial integrity: evidence from mouse and human studies

Supplemental Methods

Mouse lines and atherosclerosis models

The *Cxcr4*-floxed (*Cxcr4^{fl/fl}*) mice¹ kindly provided by Dr. Y. Zou (Columbia University, New York, US) were backcrossed into a C57Bl/6 background and crossed with C57Bl/6 *ApoE*^{-/-} mice (**Supplemental Table 1**). For tamoxifen-inducible, arterial endothelial cell-specific deletion of *Cxcr4*, *Cxcr4^{fl/fl} ApoE*^{-/-} mice were crossed with *BmxCreER^{T2}*-expressing mice² (termed *BmxCre*) kindly provided by Dr. R. Adams (MPI Münster, Germany). For smooth muscle cell (SMC)-specific deletion of *Cxcr4*, *Cxcr4^{fl/fl} ApoE*^{-/-} mice were crossed with C57Bl/6 *TaglnCre*-expressing mice (termed *TaglnCre*) to induce a constitutive knock-out of *Cxcr4* in SMCs³ (Jackson Laboratories, Bar Harbor, USA) or with C57Bl/6 *SmmhcCreER^{T2}*-expressing mice⁴ (termed *SmmhcCre*) kindly provided by Dr. S. Offermanns (MPI Bad Nauheim, Germany) to obtain mice with tamoxifen-inducible knock-out in arterial SMCs. To induce *Cxcr4* deletion, the mice were injected i.p. with tamoxifen (50 mg/kg body weight, from Sigma-Aldrich and dissolved in Miglyol, Caelo) for 5 consecutive days. A recovery period of minimal 2 weeks after the first tamoxifen injection was allowed before the start of high-fat diet (HFD) feeding. VE-PTP-FRB*/VE-cadherin-FKBP C57Bl/6 knock-in mice, expressing VE-cadherin-FKBP and VE-PTP-FRB* under the specific control of the VE-cadherin promoter, thereby replacing endogenous VE-Cadherin, were as described⁵. The VE-cadherin-FKBP fusion protein contains the rapamycin-binding domain of the FK506 binding protein (FKBP) fused to the C-terminus of VE-cadherin. The VE-PTP-FRB* fusion protein contains an HA-tagged mutated form of the rapamycin binding domain of mammalian target of rapamycin (FRB_{T2098L} = FRB*) fused to the C-terminus of VE-PTP. Treatment of these mice with a non-immunosuppressive rapamycin analogue (rapalog) that does not bind endogenous target of rapamycin (AP21967; ARIAD Pharmaceuticals Inc.) stabilizes the interaction between the VE-cadherin and VE-PTP fusion proteins by simultaneously binding to FKBP and FRB*⁵. Surgery was performed under anesthesia, and every effort was made to minimize suffering.

Bone marrow transplantation

Bone marrow (BM) cells (3×10⁶/mouse) from *TaglnCre+ Cxcr4^{fl/fl} ApoE*^{-/-} mice or from *TaglnCre- Cxcr4^{fl/fl} ApoE*^{-/-} littermate controls were flushed from femur and tibia cavities and subsequently administered to C57Bl/6

ApoE^{-/-} recipient mice by lateral tail vein injection one day after a lethal dose of whole-body irradiation (2x 6.5 Gy). The same procedure was performed with bone marrow from *BmxCre*⁻ *Cxcr4*^{fl/fl} *ApoE*^{-/-} vs *BmxCre*⁺ *Cxcr4*^{fl/fl} *ApoE*^{-/-} mice. After four weeks of recovery, the mice were placed on HFD for up to 14 weeks. For the *BmxCre* *Cxcr4*^{fl/fl} *ApoE*^{-/-} transplantation model, tamoxifen treatment (50 mg/kg body weight, i.p.) was performed for 5 consecutive days following an initial HFD of 6 weeks.

Analysis of atherosclerotic lesion using histology and immunofluorescent staining

For analysis of mouse atherosclerotic lesions, the aortic root and thoraco-abdominal aorta were stained for lipid depositions with Oil-Red-O. In brief, hearts with aortic root were embedded in Tissue-Tek O.C.T. compound (Sakura) for cryo-sectioning. Atherosclerotic lesions were quantified in 5 µm transverse sections and averages were calculated from 3-5 sections. The aorta was opened longitudinally, mounted on glass slides and *en face*-stained with Oil-Red-O. Aortic arches with main branch points (brachiocephalic artery, left subclavian artery and left common carotid artery) were fixed with 4% paraformaldehyde and embedded in paraffin. Lesion size was quantified after HE-staining of 3 transverse sections. For analysis of the cellular composition or inflammation of atherosclerotic lesions, sections were stained with an antibody to Mac2 (AbD Serotec), smoothelin (N-15, Santa Cruz), SMA (Dako), VWF (DAKO, clone: F8186), or ICAM-1 (BD pharmingen, clone: 3E2). SM22 expression was analyzed using antibody from Abcam (ab14106). SMC phenotype was analyzed by costaining for SMA (DAKO) and vimentin (Sigma, clone: LN-6), CD248 (clon&D, clone: 458606), CD68 (ebioscience, clone: kp1) or lipids using Nile Red (Sigma-Aldrich). Nuclei were counter-stained by 4',6-Diamidino-2-phenylindol (DAPI). After incubation with a secondary FITC- or Cy3-conjugated antibody (Life Technologies), sections were analyzed using a Leica DMLB fluorescence microscope and charge-coupled device (CCD) camera. TUNEL staining was performed using the In Situ Cell Death Detection Kit (Roche). Collagen was stained using Sirius Red⁶. Blinded image analysis was performed using Diskus, Leica Qwin Imaging (Leica Lt.) or Image J software. For each mouse and staining, 2-3 root sections were analyzed and data were averaged.

Human carotid artery endarterectomy specimen or autopsy samples were obtained from the Department of Pathology at Academic Medical Center Amsterdam were immediately fixed in 10% formalin and processed for paraffin embedding. All use of tissue was in agreement with the “Code for Proper Secondary Use of Human Tissue in the Netherlands”. For immunohistochemistry, antibodies against CXCR4 (Abcam, ab124824), active (non-phosphorylated) β-Catenin (ABC; Millipore 8E7), CD31 (=PECAM-1; Santa Cruz, sc-1506) and SMA (Dako, M0851, clone 1A4; or Abcam, ab5694) were used in combination with biotin-coupled or HRP-coupled secondary antibodies (rabbit anti-goat Ig, Dako, e0466; Biotin-SP AffiniPure Donkey anti-mouse IgG, Jackson

ImmunoResearch, 715-065-150; Brightvision poly-HRP anti-rabbit, Immunologic, DPVR55HRP), followed by a visualization using the avidin-biotin complex method with either alkaline phosphatase or HRP as enzyme (Vectastain ABC elite HRP Kit PK-6100 or Vectastain ABC-AP staining Kit AK-5000, both Vector) and DAB+ (Dako, K3468) or ImmPACT Vector Red Alkaline Phosphatase Substrate SK-5105 (Vector Laboratories, Braunschweig, Germany) as substrate. Cells were counter-stained by Mayer's hemalaun.

Flow cytometry

For flow cytometry analysis, whole blood obtained from the retro-orbital plexus of mice was EDTA-buffered and subjected to red blood cell lysis. Leukocyte subsets were analyzed using the following combination of surface markers: neutrophils (CD45⁺CD11b⁺CD115⁻Gr1^{high}), monocytes (CD45⁺CD11b⁺CD115⁺), classical monocytes (GR1^{high} monocytes), non-classical monocytes (GR1^{low} monocytes), T-cells (CD45⁺CD3⁺), B-cells (CD45⁺CD19⁺). Circulating angiogenic early outgrowth cells were characterized by flow cytometry using an antibody cocktail against Sca1 (Ly6A/E, clone D7, BD Biosciences), Flk1 (CD309, clone Avas12a1, eBioscience) and CD31 (clone 390, Abcam)⁷⁻⁹. Lin⁻Sca1⁺ progenitor cells were determined after staining with an anti-Sca1 antibody (clone D7, BD Biosciences) and a mouse lineage panel (CD3ε, CD11b, CD45R, GR1, TER119, Ly-6G, BD Pharmingen). CXCR4 surface expression was quantified after staining with an anti-CXCR4 antibody (clone 2B11/CXCR4, BD Biosciences). Cell populations and marker expression were analyzed using a FACSCanto-II, FACSDiva software (BD Biosciences) and the FlowJo analysis program (Treestar).

Intravital microscopy

The right jugular vein was cannulated with a catheter for antibody and dye injection. After exposure of the left carotid artery, antibodies (1 µg) to CD11b (650NC, eBioscience), Ly6G (BioLegend) and Ly6C (eBioscience) were sequentially administered to label various leukocyte subsets. Recordings were made 3 min after injection of each antibody. Finally, rhodamine 6G (100 µl, 0.1% solution) was injected to label all circulating leukocytes. Intravital microscopy was performed using an Olympus BX51 microscope equipped with a Hamamatsu 9100-02 EMCCD camera and a 10x saline-immersion objective. For image acquisition and analysis, Olympus Cell-R software was used. For induction of inflammation, carotid arteries were locally pre-treated with TNFα (100 ng).

***In vivo* Evans blue permeability assay**

For analysis after HFD, mice were injected *i.v.* with 100 µl of a 1% Evans blue solution in PBS and sacrificed after 30 min. For mice on chow diet, 10 µg of histamine (in PBS) was injected *i.v.* 25 min after Evans blue injection and 10 min before sacrifice. Mice were pretreated with the CXCR4 antagonist AMD3465 (125 µg/mouse in

PBS, for 12 h), with CXCL12 (3 μ g/mouse in PBS, for 4 h), or with Rapalog (250 μ g/mouse in vehicle, for 4 h). Lyophilized rapalog (AP21967, ARIAD Pharmaceuticals) was diluted in ethanol to prepare a 62.5 mg/ml stock solution. Mice were injected with freshly prepared rapalog using 4% of the rapalog stock solution, 10% PEG-400 (Sigma-Aldrich) in 1.7% Tween-20 (Merck) in dH₂O. After sacrifice, the aortic arch including its main branching points was carefully isolated and after washing with PBS, the amount of Evans blue that permeated into the vessel wall was quantified using ImageJ software.

Endothelial and smooth muscle cell culture *in vitro*

Human aortic endothelial cells (hAoECs, Lonza) were used between passages 4 and 10. hAoECs were cultured using Endothelial Cell Growth Medium MV (Promocell) or DMEM with 1% Nutridoma SP (Roche). For serum-starved conditions, hAoECs were washed with PBS and incubated in Endothelial Cell Basal Medium MV with 0.5% FCS, or in DMEM with 0.1% Nutridoma SP. SV-40-transformed mouse endothelial cells (SVECs) were cultured in DMEM with 5% FCS. Human aortic vascular smooth muscle cells (hVSMCs, Lonza) were used between passages 4 and 12 and cultured using Smooth Muscle Cell Growth Medium 2 (Promocell). Alternatively, they were derived from tissue explants¹⁰ and cultured in M199 medium (Gibco; Invitrogen) supplemented with 20% FCS. Cells were stimulated with CXCL12 α (Peprotech) or, where indicated, protease-resistant S-CXCL12 α (S4V)^{11,12}, TNF- α (Peprotech), WNT3a (Peprotech or R&D), LiCl, TGF- β (Peprotech), PDGF-BB (Sigma-Aldrich), and pretreated with the CXCR4 antagonists AMD3465 (Tocris) or AMD3100 (Sigma), the WNT inhibitor endo-IWR1 (Santa Cruz), the AKT inhibitor SH-5 (Santa Cruz), the SHP2 inhibitor PHPS1 (Sigma) or a PTP1B inhibitor (Calbiochem, 539749) for 30-120 min, using concentrations as indicated.

siRNA silencing

siRNAs targeting β -catenin and CXCR4 siRNA and a non-specific siRNA without target in the human transcriptome (**Supplemental Table 2**) were generated by Qiagen. For transfection, cells were trypsinized, resuspended in 100 μ l PBS, mixed with siRNA (20 nM per sample) and electroporated using Nucleofector technology (Lonza). Cells were re-plated and cultured for 24 h before stimulation.

Gene expression studies using quantitative real-time PCR

RNA was isolated using RNeasy kits and TissueLyser (both Qiagen) for disruption and homo-genization. DNase digestion was performed by RNA isolation on columns (Qiagen). cDNA was reverse transcribed from RNA using MMLV reverse transcriptase (Promega). Quantitative real-time PCR was performed using the Sybgreen technology (Maxima SYBR green/Rox qPCR Master Mix from Fermentas; LightCycler-FastStart DNA Master SYB R Green I Kit from Roche Applied Science) or using pre-developed TaqMan assays (Life Technologies).

Real-time PCR reactions with primer pairs summarized in **Supplemental Table 3** were performed using the ViiA7 Real Time PCR System (Life Technologies) or a LightCycler (Roche Applied Science). Gene expression was normalized to *GAPDH* using the $\Delta\Delta C_t$ method.

Transcription-based reporter assay of WNT/ β -Catenin signaling.

The activity of the WNT/ β -catenin signaling pathway culminating in TCF/LEF-dependent regulation of target gene transcription, was monitored in hAoECs using a reporter assay. This assay was based on a β -catenin-activated reporter (BAR) system containing multi-merized TCF/LEF DNA-binding sites and the control reporter “found-unresponsive BAR” (fuBAR) that harbors mutant TCF-binding sites. We modified the BAR/fuBAR system by inserting Gaussia luciferase as a reporter gene. Following its transcription activated by β -catenin, Gaussia luciferase is secreted into the supernatant to allow for its detection¹³.

BAR/fuBAR-transfected hAoECs were used for stimulation and/or for knockdown experiments. Conditioned media was collected after indicated periods and analyzed for the presence of reporter protein, using the Gaussia luciferase assay kit (New England Biolabs) and a plate luminometer (Tecan). No Gaussia luciferase activity was detected in conditioned media from hAoECs transfected with the fuBAR system.

***In vitro* permeability assay**

Before onset of stimulation, monolayer integrity was assessed by non-fluorescent live cell staining. Medium was refreshed and appropriate stimuli were added for indicated periods. Endothelial permeability was measured by addition of a FITC-Dextran solution into the insert and quantification of the permeated FITC-Dextran in the bottom well using a fluorescence plate reader (Tecan).

***In vitro* scratch assay**

HAoSMCs were grown to confluency and were left untreated or were pre-stimulated for 21 h with CXCL12 (100 ng/ml) or AMD3100 (1 μ g/ml), as indicated. For each well, 10 consecutive pictures were recorded by phase contrast microscopy at the start and after 15 h of the migration, overlaid, and the number of cells migrating into the wound area was quantified using Image J software.

Protein lysates and western blot analysis

Cell pellets from *in vitro* stimulation experiments for western blot analysis were lysed in RIPA lysis buffer (Pierce) containing protease inhibitors (Complete Protease Inhibitor Cocktail, Roche) and phosphatase inhibitors (PhosSTOP, Roche). Mouse vessels were lysed in RIPA lysis buffer containing protease inhibitors (Complete Protease Inhibitor Cocktail, Roche) and phosphatase inhibitors (PhosSTOP, Roche) using a TissueLyser (Qiagen)

for tissue disruption and homogenization. Cytoplasmic and nuclear extracts were isolated separately using a subcellular fractionating buffer (Abcam). Protein concentrations were determined using the DC Protein Assay (BioRad). SDS/polyacrylamide gel electrophoresis and Western blotting were performed according to standard protocols. For analysis of *in vitro* cultures of human cells, primary antibodies were used against β -catenin (Cell signaling, 9582S), lamin B1 (Santa Cruz, sc-20682), tubulin (Abcam, ab6046) and VE-cadherin (ebioscience, eBioBV13). For analysis of mouse samples, primary antibodies to PCNA (Cell signaling, #2586), ApoA1 (Meridian Life Science, K23500R), VE-cadherin (Abnova, H00001003-A01) and β -actin (Abcam, ab8227) were used. Bound antibodies were visualized with the enhanced chemiluminescence (ECL) system (Pierce or GE Healthcare). Densitometry quantification of bands was performed using a GS-800 Calibrated Densitometer driven by Quantity One 1-D Analysis software (Bio-Rad Laboratories, Hercules, CA, USA) or Image J analysis software. Recombinant protein standards (Invitrogen) were used for molecular mass determination.

Immunocytochemistry

The subcellular localization of β -catenin protein in hAoECs was examined by immunocytochemistry. Culture slides were incubated with mouse anti- β -catenin antibodies (Santa Cruz Biotechnology) at a dilution of 1:500 in a solution containing 0.5% Triton X-100 and 10% normal goat serum for 2 h at 37°C. After several washes in PBS, the culture slides were incubated with rhodamine-conjugated anti-rabbit IgG-R (Santa Cruz Biotechnology) at a dilution of 1:500 for 45 min. Nuclei were counter-stained by 4',6-Diamidino-2-phenylindol (DAPI). Stained cells were visualized using a fluorescent microscope.

Surface marker analysis on cultured cells

CXCR4 surface expression was analyzed on hAoECs and VSMCs by flow cytometry using the CXCR4 antibody (BD Pharmingen, 555974), as compared to isotype control. VCAM-1 surface expression was measured on SVECs using a fluorescence plate reader after staining the cells with an anti-VCAM1-PE antibody (ebioscience clone 429).

Vascular reactivity in organ chambers and plasma nitrite measurement

Rings were contracted with KCl (80 mmol/L) three times. After washing, phenylephrine was added in cumulative concentrations to a tension of 80% of maximal KCl contraction. After stabilization for 10 min, acetylcholine or the NO donor DETA-NONOate were added at cumulative concentrations to trigger endothelium-dependent and -independent relaxation, respectively. Data were expressed as percentage of the initial Phe-induced contraction (80% of maximal KCl contraction). In other experiments, phenylephrine was added to reach a contraction of 10% of maximal KCL contraction followed by adding L-nitro-arginine methyl ester (L-NAME, 300 μ mol/L) to

the chamber. Data were expressed as the ratio of L-NAME-induced contraction to basal pre-contraction without L-NAME. To determine plasma nitrite levels, blood was collected by cardiac puncture and anticoagulated with heparin. Plasma proteins were precipitated by mixing plasma with 10% trichloroacetic acid and removed by centrifugation. The cleared supernatant was analyzed for nitrite, nitric oxide reacts with dissolved oxygen, with the aid of the NO analyzer (Sievers).

Cholesterol efflux assays

J774 cells (mouse macrophage cell line), maintained in RPMI-1640 plus 10% FBS and 0.5% gentamycin, were plated in 24-well plates and labelled overnight using 0.5 ml/well of 2 $\mu\text{Ci/ml}$ [$1,2\text{-}^3\text{H}$] cholesterol in RPMI-1640 plus 1% FBS. After washing, cells were equilibrated for 4 h in RPMI-1640 equilibration medium containing 0.2% BSA and 0.5% gentamycin including 0.3 mM Cpt-cAMP (Sigma) to upregulate ABCA1. Efflux was calculated as the fraction of total cellular cholesterol released in 3 h to ApoB-depleted serum, obtained after removal of ApoB lipoproteins with polyethylene glycol (PEG, MW 8000, Sigma) for 20 min¹⁴ and diluted to 1% final serum concentration in MEM-HEPES (0.5 ml/well). Alternatively, HDL was added as acceptor at a final concentration of 25 $\mu\text{g/ml}$ in MEM-HEPES (0.5 ml/well). As baseline for cholesterol efflux, MEM-HEPES without serum or HDL was added (0.5 ml/well). ABCA1-mediated cholesterol efflux is the difference between cAMP-treated and non-cAMP-treated J774 cells during equilibration.

Blood pressure measurements and ELISA

Blood pressure was measured non-invasively using a mouse tail blood pressure cuff. CXCL12 levels in mouse serum or plasma were measured using a mouse CXCL12/SDF-1 α ELISA kit (Ray Biotech), according to the manufacturer's protocol.

β -Galactosidase staining

Mice were anesthetized, exsanguinated and the vasculature was rinsed *in vivo* with cold phosphate-buffered saline (PBS) containing 2 mM MgCl_2 . After *in situ* perfusion with a cold 2% paraformaldehyde solution, carotid arteries, thoracic aorta, aortic arch and aortic root were isolated, fixed for 15 min on ice and washed three times. Samples were incubated overnight at 37°C in a pre-warmed β -gal staining solution, containing 1 mg/ml of the substrate X-gal in an X-gal reaction buffer (PBS containing 5 mM potassium ferro-cyanide, 5 mM potassium ferricyanide, 2 mM MgCl_2 , 0.02 % Nonidet P-40 and 0.01% Na-deoxycholate). The next day, the samples were rinsed with PBS until the washing buffer no longer turned yellow. The stained samples were then embedded in Tissue-Tek O.C.T. compound (Sakura) for 2 h and cryosections were prepared. β -galactosidase staining was visualized using light microscopy.

Analysis of CXCR4 in humans

We examined the association of 345 common variants at the CXCR4 locus (\pm 25KB) with CHD by using data on 92,516 CHD cases and 167,280 controls (see **Supplemental Table 4** for details of data sets included), most notably interrogating the CARDIoGRAMplusC4D (Coronary ARtery DIsease Genome wide Replication and Meta-analysis plus The Coronary Artery Disease [C4D] Genetics) data in a logistic regression analysis, as described.¹⁵ We conducted fine-mapping studies in 12,500 myocardial infarction cases and 12,000 controls and genotyped all 512 variants with a MAF $>0.1\%$ identified by the 1000-Genomes project at the CXCR4 locus. Common variant analyses were declared to be significant at a P-value of 5×10^{-5} after Bonferroni correction for 857 variants, and eQTL analysis of whole blood was performed (Saleheen et al., in preparation). The SNPs were genotyped using a conventional GWAS/metabochip array by the studies participating in CARDIoGRAMplusC4D and other additional studies. Analyses were conducted employing an additive model. For every C allele at rs2322864, the OR for CHD was found to be 1.04; $P=4.38 \times 10^{-7}$. For meta-analysis, we used an inverse variance-based approach, as described.¹⁶ Quantification of CXCR4 mRNA expression and genotyping of rs2322864 in the human plaque specimens using a homogenous fluorescent method and melting-curve analysis was performed, as described¹⁷⁻¹⁹ and correlated with the clinical phenotype, either defined by asymptomatic stable atherosclerosis or by symptomatic disease, as apparent by cerebral ischemic events, e.g. transient ischemic attacks or stroke. In this small cohort (n=188), the allele frequency was skewed in favor of the minor allele and the overall numbers were lower so that we also opted to test for effects in a recessive model. To adjust the P-values for the number of models tested, we used Bonferroni correction for multiple comparisons. The genotypes were distributed in agreement with a Hardy-Weinberg equilibrium ($P=0.19$).

Statistics

All data are expressed as mean \pm SD or mean \pm SEM, as indicated. Statistical analyses were performed using GraphPad Prism 6 (GraphPad Software Inc.). After testing for normality, unpaired Student's t-test (with Welch correction for animal experiments), Mann-Whitney test, one-way ANOVA with Tukey's or Sidak's multiple comparison test, Kruskal-Wallis test with Dunn's multiple comparisons test, or 2-way ANOVA or 2-way repeated measures ANOVA with Bonferroni post-test were used, as appropriate. P-values < 0.05 were considered as being statistically significant.

Supplemental Tables

Supplemental Table 1: Mouse gender in experimental models

Mouse lines and experimental models	Age (weeks) at start	Gender	Blinded fashion	Comments	Figure
<i>BmxCre</i> ⁺ <i>Cxcr4</i> ^{fl/fl} <i>ApoE</i> ^{-/-} 12 weeks HFD	~8	female	yes	Females were used for comparison with the <i>TaglnCre</i> study	1 A-L
<i>TaglnCre</i> ⁺ <i>Cxcr4</i> ^{fl/fl} <i>ApoE</i> ^{-/-} 12 weeks HFD	~8	female	yes	Females were used as complementary study to the <i>SmmhcCre</i> study	2 A-H
<i>SmmhcCre</i> ⁺ <i>Cxcr4</i> ^{fl/fl} <i>ApoE</i> ^{-/-} 12 weeks HFD	~8	male	yes	Because the <i>SmmhcCre</i> gene is located on the y-chromosome, only males were used for these experiments.	2 I-O
<i>TaglnCre</i> ⁺ <i>Cxcr4</i> ^{fl/fl} <i>ApoE</i> ^{-/-} BMT + 12 weeks HFD	~8	female	yes	Females were used for comparison with the <i>TaglnCre</i> HFD study	S3 H-M
<i>BmxCre</i> ⁺ <i>Cxcr4</i> ^{fl/fl} <i>ApoE</i> ^{-/-} BMT + 14 weeks HFD	~8	female	yes	Females were used for comparison with the <i>BmxCre</i> HFD study	S3 A-G
C57/Bl6 AMD/CXCL12 + EVB	~8	female	yes		3 A-D
<i>BmxCre</i> ⁺ <i>Cxcr4</i> ^{fl/fl} <i>ApoE</i> ^{-/-} 12 weeks HFD + Evans blue	~8	mixed	yes	Both genders were used to provide evidence for a gender-independent mechanism.	3 E-G
VE-PTP-FRB ⁺ /VE-cadherin-FKBP C57/Bl6 AMD + Evans blue	~8	mixed	yes	Both genders were used to provide evidence for a gender-independent mechanism.	4 I-K
<i>BmxCre</i> ⁺ <i>Cxcr4</i> ^{fl/fl} <i>ApoE</i> ^{-/-} intravital microscopy	~8	male	yes	Because of their size at this age, male mice are slightly better suited for this experimental setup.	1 M-N
<i>BmxCre</i> ⁺ <i>Cxcr4</i> ^{fl/fl} <i>ApoE</i> ^{-/-} vascular reactivity	~8	males	yes	Males were used for comparison with the <i>SmmhcCre</i> vascular reactivity study	S5 A-C
<i>TaglnCre</i> ⁺ <i>Cxcr4</i> ^{fl/fl} <i>ApoE</i> ^{-/-} vascular reactivity	~8	males	yes	Males were used for comparison with the <i>SmmhcCre</i> vascular reactivity study	5 D-F S5 J-N
<i>SmmhcCre</i> ⁺ <i>Cxcr4</i> ^{fl/fl} <i>ApoE</i> ^{-/-} vascular reactivity	~8	males	yes	Because the <i>SmmhcCre</i> gene is located on the y-chromosome, only males were used for these experiments.	S5 O-Q

Supplemental Table 2: Sequences used for gene silencing

siRNA	Sense sequence	Antisense sequence
control	UUCUCCGAACGUGUCACGUdTdT	ACGUGACACGUUCGGAGAAAdTdT
β -catenin	UGGUUGCCUUGCUCACAATT	UUGUUGAGCAAGGCAACCATT
CXCR4	CCGACUUCAUCUUUGCCAATT	UUGGCAAAGAUGAAGUCGGGA

Supplemental Table 3: Primer sequences or Taqman assay used for real time-PCR

Gene (human)	Primer sequence or Taqman assay ID
MT1-MMP	LightCycler Primer Set (Search LC), Qiagen
Cyclin-D1	LightCycler Primer Set (Search LC), Qiagen
AXIN-2	LightCycler Primer Set (Search LC), Qiagen
VE-Cadherin	LightCycler Primer Set (Search LC), Qiagen
GAPDH	LightCycler Primer Set (Search LC), Qiagen
β -catenin (CTNNB1)	Hs00355049_m1
JAM-A (F11R)	Hs00170991_m1
ESAM	Hs00332781_m1
CLDN1	Hs00221623_m1
CLDN2	Hs00252666_s1
CLDN3	Hs00265816_s1
CLDN4	Hs00976831_s1
CNN1	Hs00154543_m1
Smoothelin	Hs00199489_m1
Tagln	Hs01038777_g1
TNF- α	Hs01113624_g1
Vimentin	Hs00958111-m1
MCP-1 forward	GATCTCAGTGCAGAGGCTCG
MCP-1 reverse	TGCTTGCCAGGTGGTCCAT
ICAM-1 forward	GCTCCTGCCTGGGAACAACCG
ICAM-1 reverse	GGGGAGGGGTGCCAGTTCCA
VCAM-1 forward	TGTGCCCACAGTAAGGCAGGC
VCAM-1 reverse	AGCTGGTAGACCCTCGCTGGA
E-selectin forward	GCCACAGGACACTGGTCTGGC
E-selectin reverse	GGCAGCTGCTGGCAGGAACA
eNOS	Hs01574659_m1
GAPDH	4333764
Gene (mouse)	Taqman assay ID
CD248	Mm00547485_s1
SMA	Mm00725412_s1
Smoothelin	Mm00443013_m1
Tagln	Mm00441661_g1
Vimentin	Mm01333430_m1
18sRNA	Mm03928990_g1

Supplemental Table 4: Human data sets used for common variant analysis

Study	Full Name	Pubmed ID
CARDIoGRAMplusC4D	Coronary ARtery Disease Genome wide Replication and Meta-analysis (CARDIoGRAM) plus The Coronary Artery Disease (C4D) Genetics	26343387
CIHDS & CGPS	Copenhagen Ischemic Heart Disease Study, Copenhagen General Population Study	17635890, 18523221, 18971492, 19509380
CCHS	Copenhagen City Heart Study	16575269
PROMIS & BRAVE	Pakistan Risk of Myocardial Infarction Study, The Bangladesh Risk of Acute Vascular Events	19404752 & 25930055
ARIC_MALE	Atherosclerosis Risk in Communities_male	2646917, 10472985
ARIC_FEMALE	Atherosclerosis Risk in Communities_female	2646917, 10472985
WHI	Womans Health Initiative	9492970, 16467234
MIGEN – AA	Myocardial Infarction Genetics	15234427, 26934567
TAICHI	Taiwan-MetaboChip Study for Cardiovascular Disease	23555291
MALMO	Malmö Diet and Cancer study	10809998, 2018027, 8429286
Ruth – EA	https://www.ottawaheart.ca/research-team/ruddy-canadian-cardiovascular-genetics-centre	
OHGS_B2	Ottawa Heart Genomics Study	20670758, 19885677
OHGS_A2	Ottawa Heart Genomics Study	20670758, 19885677
OHGS_C2	Ottawa Heart Genomics Study	20670758, 19885677
CCGB_2	Cleveland Clinic GeneBank	20670758
German-MI	German myocardial infarction familiiy study	11818963
Mayo-MI	Mayo Clinic Olmsted County population-based cohort with myocardial infarction	26699392, 27437886

Details and references of human data sets used for common variant analysis, as displayed in the forest plot shown in **Figure 6D**.

Supplemental Table 5: Blood parameters of *BmxCre⁺Cxcr4^{fl/fl}* vs *BmxCre⁻Cxcr4^{fl/fl} Apoe^{-/-}* mice

	<i>SmmhcCre⁺Cxcr4^{fl/fl} Apoe^{-/-}</i>	<i>SmmhcCre⁻Cxcr4^{fl/fl} Apoe^{-/-}</i>	P-value
Cholesterol (mg/dL)	2100 ± 970	2089 ± 883	0.731
Triglycerides (mg/dL)	255 ± 134	215 ± 195	0.171
Body weight (g)	35.2 ± 4.3	34.1 ± 4.4	0.496
Platelets (x 10 ³ /μl)	1041 ± 316	901 ± 359	0.288

Listed are serum levels of cholesterol and triglycerides, body weight and platelet numbers in peripheral blood of *BmxCre⁺Cxcr4^{fl/fl} Apoe^{-/-}* vs *BmxCre⁻Cxcr4^{fl/fl} Apoe^{-/-}* mice after 12 weeks of high-fat diet (HFD). Data represent mean±SD of 13-20 mice. P-values by Student's t-test with Welch correction or Mann-Whitney test, as appropriate.

Supplemental Table 6: Blood parameters of *TaglnCre⁺Cxcr4^{fl/fl}* vs *TaglnCre⁻Cxcr4^{fl/fl} Apoe^{-/-}* mice

	<i>TaglnCre⁺Cxcr4^{fl/fl} Apoe^{-/-}</i>	<i>TaglnCre⁻Cxcr4^{fl/fl} Apoe^{-/-}</i>	P-value
Cholesterol (mg/dL)	1062 ± 499	690 ± 213	0.033
Triglycerides (mg/dL)	226 ± 112	128 ± 25	0.003
Body weight (g)	27.5 ± 3.1	25.5 ± 2.7	0.082
Platelets (x 10 ³ /μl)	670 ± 66	681 ± 50	0.551

Listed are serum levels of cholesterol and triglycerides, body weight and platelet numbers in peripheral blood of *TaglnCre⁺Cxcr4^{fl/fl} Apoe^{-/-}* vs *TaglnCre⁻Cxcr4^{fl/fl} Apoe^{-/-}* mice after 12 weeks of HFD. Data represent mean±SD of 6-16 mice. P-values by Student's t-test with Welch correction or Mann-Whitney test, as appropriate.

Supplemental Table 7: Blood parameters of *SmmhcCre*⁺ vs *SmmhcCre*⁻*Cxcr4*^{fl/fl}*Apoe*^{-/-} mice

	<i>SmmhcCre</i> ⁻ <i>Cxcr4</i> ^{fl/fl} <i>Apoe</i> ^{-/-}	<i>SmmhcCre</i> ⁺ <i>Cxcr4</i> ^{fl/fl} <i>Apoe</i> ^{-/-}	P-value
Cholesterol (mg/dL)	2100 ± 970	2089 ± 883	0.731
Triglycerides (mg/dL)	255 ± 134	215 ± 195	0.171
Body weight (g)	35.2 ± 4.3	34.1 ± 4.4	0.496
Platelets (x 10 ³ /μl)	1041 ± 316	901 ± 359	0.288

Listed are plasma levels of cholesterol and triglycerides, body weight and platelet numbers in peripheral blood of *SmmhcCre*⁺*Cxcr4*^{fl/fl}*Apoe*^{-/-} vs *SmmhcCre*⁻*Cxcr4*^{fl/fl}*Apoe*^{-/-} mice after 12 weeks of HFD. Data represent mean±SD of 9-19 mice. P-values by Student's t-test with Welch correction or Mann-Whitney test, as appropriate.

Supplemental Table 8: Blood parameters of *Apoe*^{-/-} recipients after reconstitution with *BmxCre*⁺*Cxcr4*^{fl/fl}*Apoe*^{-/-} vs *BmxCre*⁻*Cxcr4*^{fl/fl}*Apoe*^{-/-} bone marrow

	BM: <i>BmxCre</i> ⁻ <i>Cxcr4</i> ^{fl/fl} <i>Apoe</i> ^{-/-}	BM: <i>BmxCre</i> ⁺ <i>Cxcr4</i> ^{fl/fl} <i>Apoe</i> ^{-/-}	P-value
Cholesterol (mg/dL)	787 ± 125	775 ± 204	0.877
Triglycerides (mg/dL)	159 ± 60	143 ± 65	0.587
Body weight (g)	23.7 ± 1.6	25.0 ± 2.7	0.229
Platelets (x 10 ³ /μl)	683 ± 107	529 ± 108	0.008
Leukocytes (x 10 ³ /μl)	4.2 ± 1.8	5.2 ± 1.7	0.237
Monocytes (% of leukocytes)	6.3 ± 1.9	4.9 ± 2.0	0.136
Neutrophils (% of leukocytes)	24.8 ± 9.6	19.5 ± 6.9	0.319
Lymphocytes (% of leukocytes)	63.5 ± 10.4	71.9 ± 5.0	0.063

Listed are serum levels of cholesterol and triglycerides, body weight and analysis of platelets, leukocytes and leukocyte subsets by differential blood count in peripheral blood of *Apoe*^{-/-} after reconstitution with *BmxCre*⁺*Cxcr4*^{fl/fl}*Apoe*^{-/-} vs *BmxCre*⁻*Cxcr4*^{fl/fl}*Apoe*^{-/-} BM and 14 weeks of HFD. Endothelial *Cxcr4* deletion was induced by tamoxifen treatment after 6 weeks of HFD. Data represent mean±SD of 8-11 mice. P-values by Student's t-test with Welch correction or Mann-Whitney test, as appropriate.

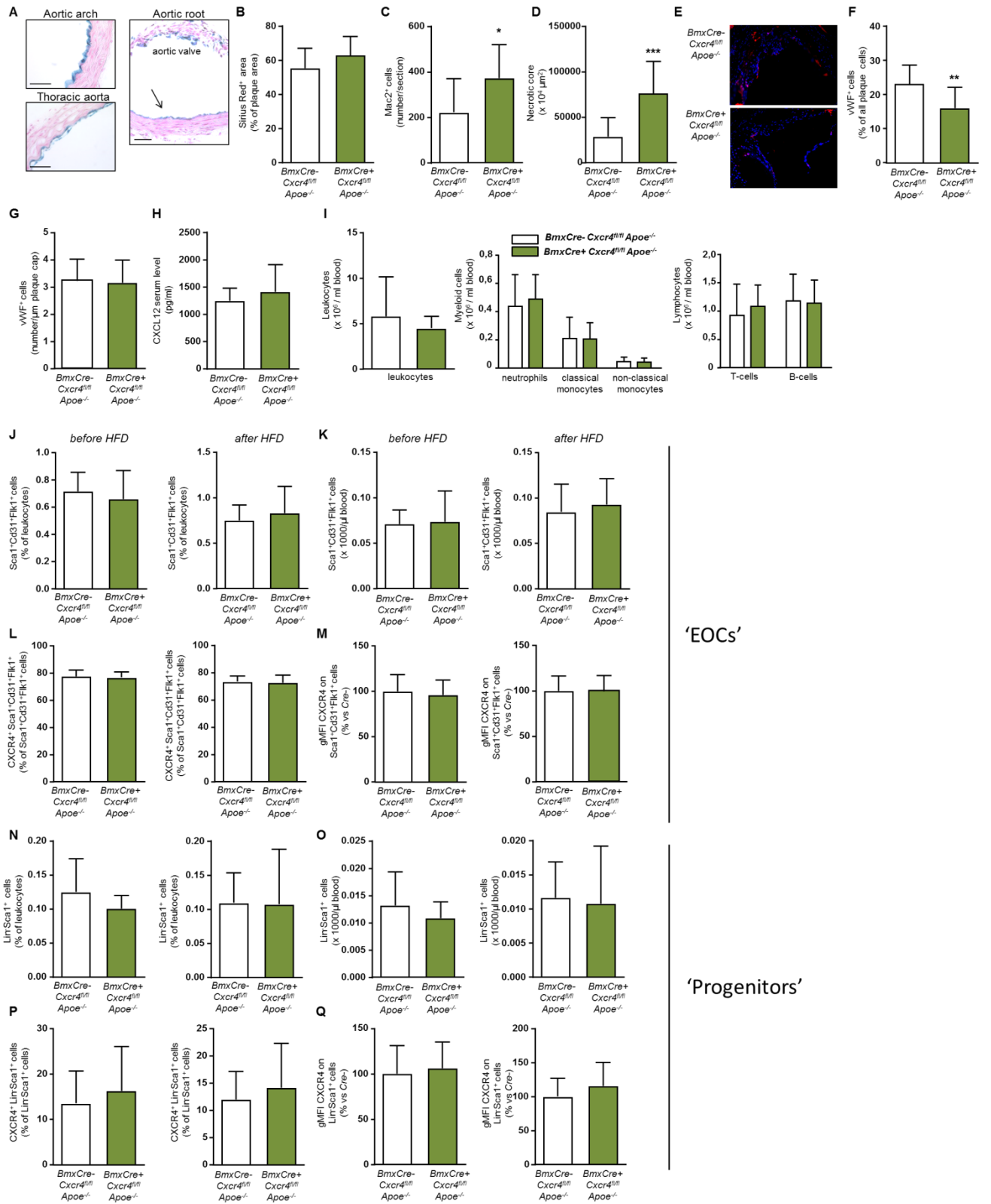
Supplemental Table 9: Blood parameters of *Apoe*^{-/-} recipients after reconstitution with *TaglnCre*⁺*Cxcr4*^{fl/fl}*Apoe*^{-/-} vs *TaglnCre*⁻*Cxcr4*^{fl/fl}*Apoe*^{-/-} bone marrow

	BM: <i>TaglnCre</i> ⁻ <i>Cxcr4</i> ^{fl/fl} <i>Apoe</i> ^{-/-}	BM: <i>TaglnCre</i> ⁺ <i>Cxcr4</i> ^{fl/fl} <i>Apoe</i> ^{-/-}	P-value
Cholesterol (mg/dL)	667 ± 122	595 ± 176	0.285
Triglycerides (mg/dL)	125 ± 77.9	109 ± 65.7	0.647
Body weight (g)	22.6 ± 2.7	22.7 ± 2.1	0.929
Platelets (10 ³ /μl)	631 ± 32	537 ± 56	0.152
Leukocytes (10 ³ /μl)	4.8 ± 1.6	5.7 ± 3.8	0.936
Monocytes (% of leukocytes)	5.7 ± 1.7	6.6 ± 1.6	0.228
Neutrophils (% of leukocytes)	25.6 ± 5.1	25.6 ± 9.8	1.000
Lymphocytes (% of leukocytes)	68.6 ± 5.4	67.7 ± 10.3	0.798

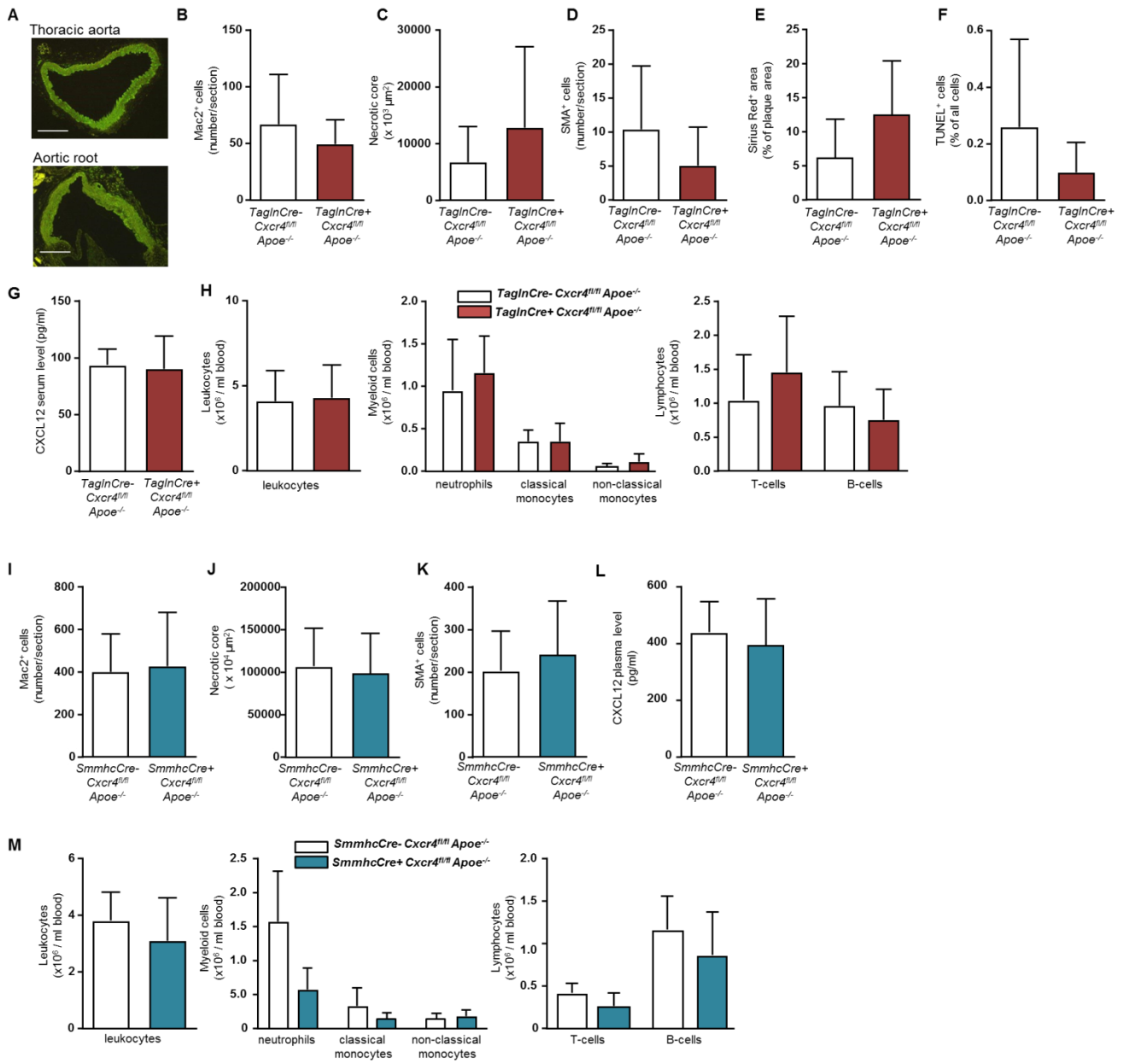
Listed are plasma levels of cholesterol and triglycerides, body weight and analysis of platelets, leukocytes and leukocyte subsets by differential blood count in peripheral blood of *Apoe*^{-/-} after reconstitution with *TaglnCre*⁺*Cxcr4*^{fl/fl}*Apoe*^{-/-} vs *TaglnCre*⁻*Cxcr4*^{fl/fl}*Apoe*^{-/-} BM and 12 weeks of HFD. Data represent mean±SD of 10-11 mice. P-values by Student's t-test with Welch correction or Mann-Whitney test, as appropriate.

Supplemental Figures

Supplemental Figure 1

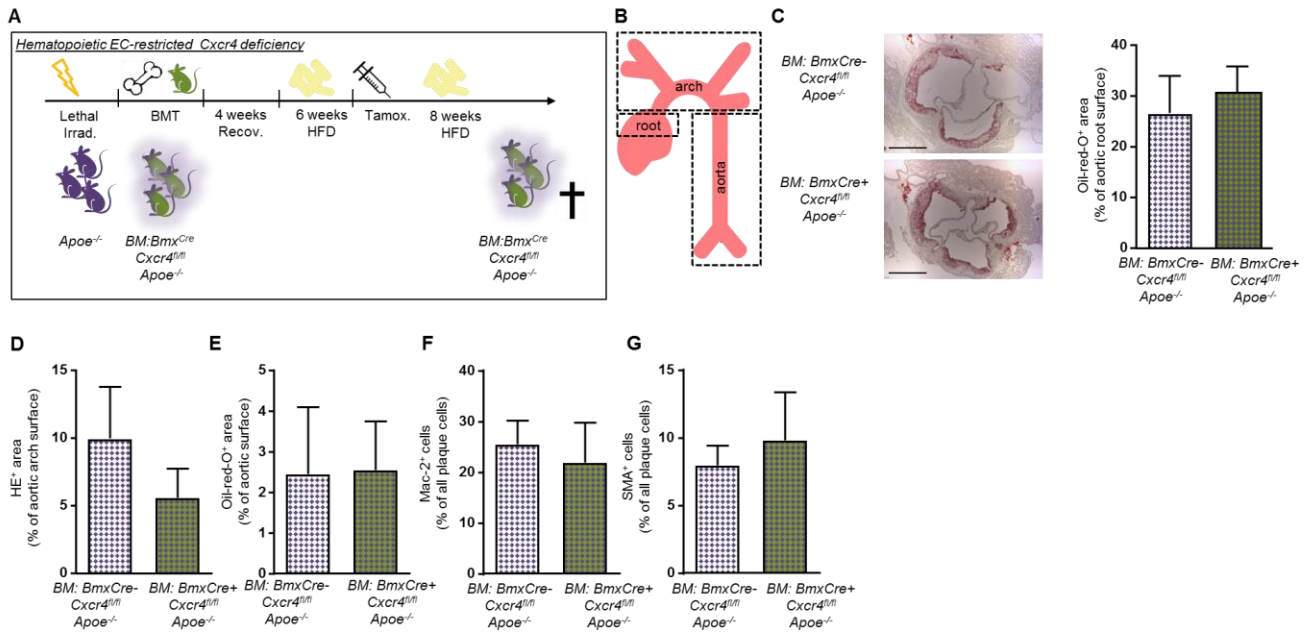


Supplemental Figure 2

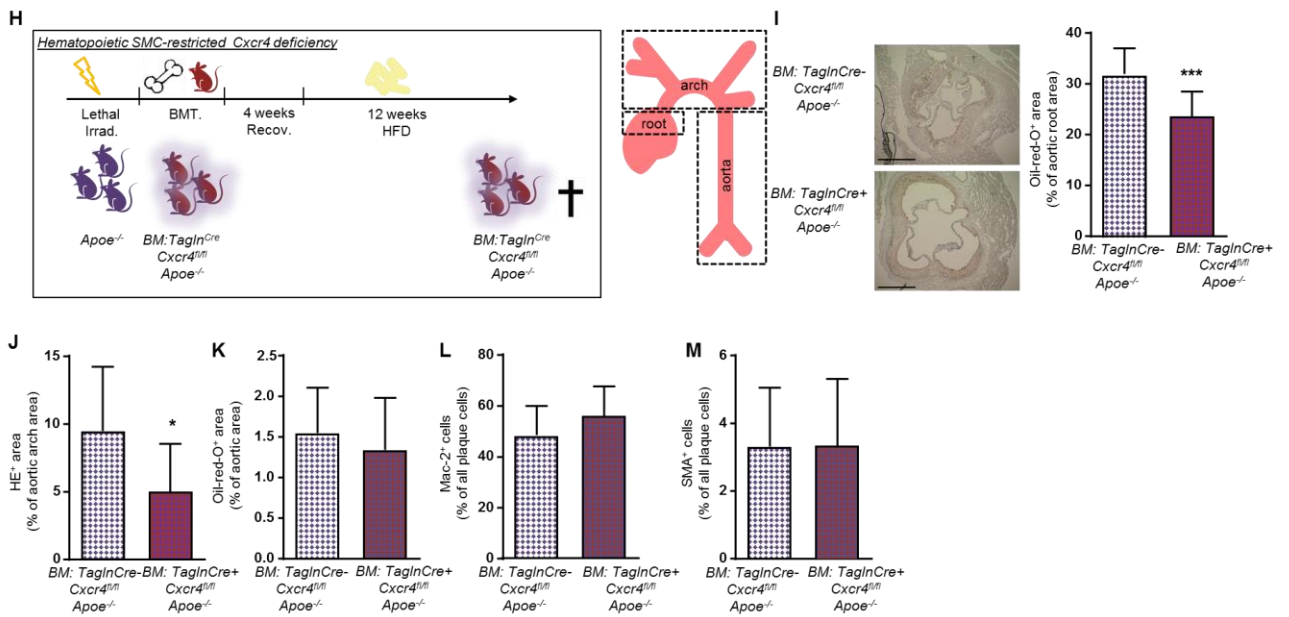


Supplemental Figure 3

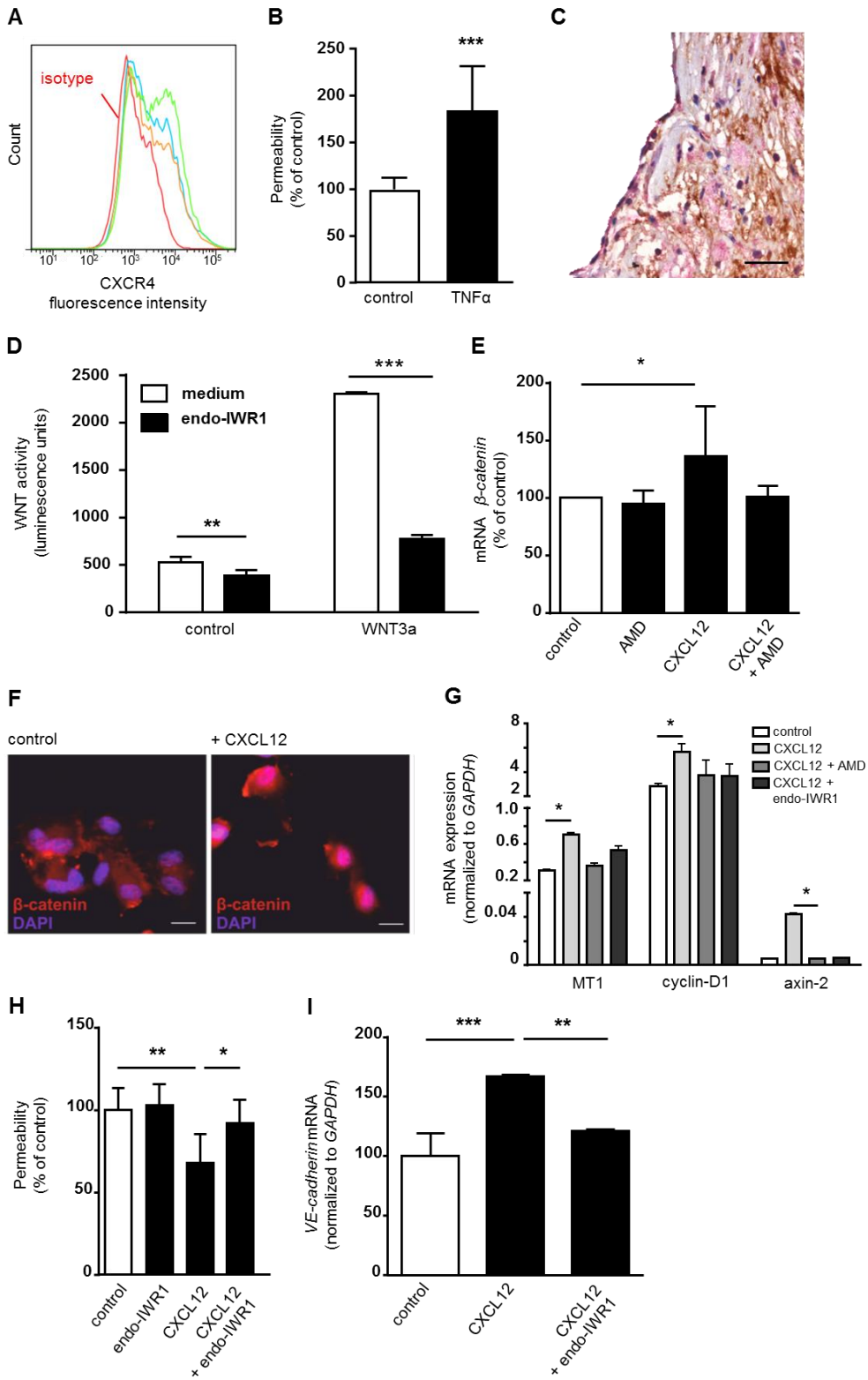
Apoe^{-/-} BmxCre Cxcr4^{fllox} – EC-specific Cxcr4 deficiency bone marrow transplantation



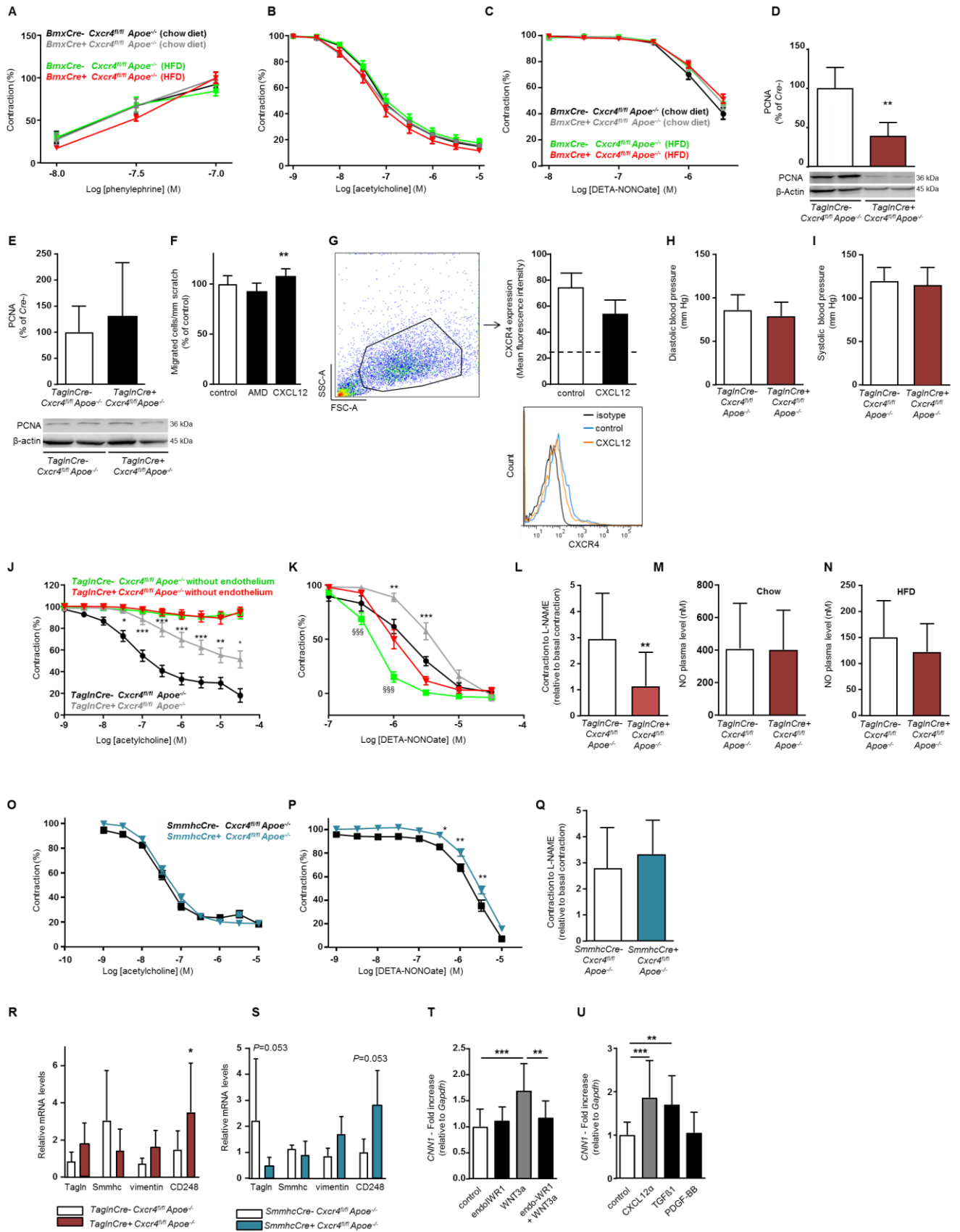
Apoe^{-/-} TaglnCre^{ERT} Cxcr4^{fllox} – SMC-specific Cxcr4 deficiency bone marrow transplantation



Supplemental Figure 4



Supplemental Figure 5



Supplemental Figure Legends

Supplemental Figure 1: Analysis of atherosclerosis and of progenitor cells in *BmxCre Cxcr4^{fl/fl} Apoe^{-/-}* mice.

(A) β -Galactosidase activity in the aortic arch, thoracic aorta and aortic root from tamoxifen-treated *BmxCreER^{T2} ROSA* reporter mice, showing activity of Bmx-driven Cre in arterial ECs. Scale bar = 50 μ m. (B-I) *BmxCre⁺ Cxcr4^{fl/fl} Apoe^{-/-}* mice and *BmxCre⁻* controls were analyzed after 12 weeks of high-fat diet (HFD). (B) Collagen content of aortic root lesions was quantified after Sirius Red staining (n=10-14). (C) Macrophage content in aortic root lesions was quantified after Mac2 staining (n=10-13). (D) Necrotic core area in aortic root lesions was determined by quantifying the anuclear area (n=12-14). (E-G) Representative pictures (E) and quantification of ECs in aortic root lesions after von Willebrand factor (VWF) staining, given as % of plaque cells (F) or (G) relative to the plaque cap length (n=12-14). (H) CXCL12 serum levels, as analyzed by ELISA (n=13-15). (I) Analysis of blood leukocytes (by counter) and subsets of neutrophils, monocytes, T- and B-cells (by flow cytometry) after 10 weeks of HFD (n=7-8). (B-I) Data represent mean \pm SD, * P <0.05; ** P <0.01, *** P <0.001 by Student's t-test with Welch correction or Mann-Whitney test, as appropriate. (J-Q) Circulating Sca1⁺CD31⁺ Flk1⁺ angiogenic early outgrowth cells (EOCs) and Lin⁻Sca1⁺ progenitor cells in peripheral blood were analyzed by flow cytometry in *BmxCre⁺ Cxcr4^{fl/fl} Apoe^{-/-}* vs *BmxCre⁻ Cxcr4^{fl/fl} Apoe^{-/-}* mice before and after 8-10 weeks of HFD, as indicated. (J-K) Relative (J) and absolute (K) levels of Sca1⁺CD31⁺Flk1⁺ cells (n=10-11), as analyzed by flow cytometry. (L-M) Quantification of CXCR4 expression on the surface of Sca1⁺CD31⁺ Flk1⁺ cells: % of CXCR4⁺ cells (L; n=10-11); and geometric MFI (gMFI) of surface CXCR4 after subtraction of FMO control (M; n=10-11). (N-O) Relative (N) and absolute (O) levels of Lin⁻Sca1⁺ cells (n=9-19). (P-Q) Quantification of CXCR4 expression on the surface of Lin⁻Sca1⁺ cells: % of CXCR4⁺ Lin⁻ cells (P before diet: n=10; after diet: n=19-21); and geometric MFI (gMFI) of surface CXCR4 after subtraction of the FMO control (Q before diet: n=10; after diet: n=19-21). Data represent mean \pm SD. Statistical analysis by Student's t-test with Welch correction or Mann-Whitney test, as appropriate.

Supplemental Figure 2: Analysis of atherosclerosis in *TaglnCreCxcr4^{fl/fl}* and *SmmhcCreCxcr4^{fl/fl} Apoe^{-/-}* mice.

(A) Immunofluorescence staining of Tagln in thoracic aorta and aortic root of *Apoe^{-/-}* mice. Representative figures are shown. Scale bar = 200 μ m. (B-H) *TaglnCre⁺ Cxcr4^{fl/fl} Apoe^{-/-}* mice and *TaglnCre⁻* controls were analyzed after 12 weeks of HFD. (B) Macrophage content in aortic root lesions was quantified after Mac2 staining (n=4-16). (C) Necrotic core area in aortic root lesions was determined by quantification of anuclear area (n=6-16). (D) Smooth muscle cell content in aortic root lesions was quantified after SMA staining, (n=5-16). (E) Collagen content of aortic root lesions was quantified after Sirius Red staining (n=6-16). (F) TUNEL⁺ apoptotic

cells in aortic root lesions (n=5). **(G)** CXCL12 serum levels, as analyzed by ELISA (serum pooled from 6-16 mice, measured in duplicate). **(H)** Analysis of blood leukocytes (by counter) and subsets of neutrophils, monocytes, T- and B-cells (by flow cytometry) (n=6-16). **(I-M)** *SmmhcCre⁺Cxcr4^{fl/fl}ApoE^{-/-}* mice and *SmmhcCre*-controls were analyzed after 12 weeks of HFD. **(I)** Macrophage content in aortic root lesions was quantified after Mac2 staining (n=12-14). **(J)** Necrotic core area in aortic root lesions was determined by quantification of anuclear area (n=12-13). **(K)** Smooth muscle cell content in aortic root lesions was quantified after SMA staining (n=12-14). **(L)** CXCL12 plasma levels, as analyzed by ELISA (n=13-15). **(M)** Analysis of blood leukocytes and subsets of neutrophils, monocytes, T- and B-cells by flow cytometry (n=9-15). **(A-M)** Data represent mean±SD. Statistical analysis by Student's t-test with Welch correction or Mann-Whitney test, as appropriate.

Supplemental Figure 3: Role of CXCR4 on bone marrow-derived ECs and SMCs in atherosclerosis. (A-G) *ApoE^{-/-}* mice were reconstituted with bone marrow (BM) from *BmxCre⁺Cxcr4^{fl/fl}* vs *BmxCre⁻Cxcr4^{fl/fl} ApoE^{-/-}* mice and fed a HFD for 14 weeks in total. After 6 weeks of HFD, mice were treated with tamoxifen to induce *Cxcr4* deletion in BM-derived *Bmx⁺* ECs. **(A)** Experimental scheme for BM transplantation, tamoxifen treatment and HFD. **(B-E)** Lesion area was measured after Oil-Red-O or HE staining in aortic roots **(B)**; n=8-11), aortic arch **(D)**; n=5) and aorta **(C)**; n=7-11). Representative pictures are shown for aortic root. Scale bars = 500 µm. **(F)** Macrophage content in aortic root lesions was quantified after Mac2 staining (n=8-11). **(G)** Smooth muscle cell content in aortic root lesions was quantified after SMA staining (n=7-10). **(H-M)** *ApoE^{-/-}* mice transplanted with bone marrow (BM) from *TaglnCre⁺Cxcr4^{fl/fl}ApoE^{-/-}* vs *TaglnCre⁻Cxcr4^{fl/fl}ApoE^{-/-}* mice were analyzed after 12 HFD. **(H)** Experimental scheme for BM transplantation and HFD. **(I-M)** Lesion area was measured after Oil-Red-O and HE staining in the aortic root **(I)**; n=11), aortic arch **(J)**; n=7-9) and aorta **(K)**; n=11). Representative pictures are shown for aortic root. Scale bars = 500 µm. **(L)** Macrophage content in aortic root lesions was quantified after Mac2 staining (n=10). **(M)** Smooth muscle cell content in aortic root lesions was quantified after SMA staining (n=10). **(B-M)** Data represent mean±SD. **P*<0.05, ****P*<0.001 by Student's t-test with Welch correction or Mann-Whitney test, as appropriate.

Supplemental Figure 4: Functional role of CXCR4 in endothelial cells. (A) CXCR4 surface expression intensity analyzed by flow cytometry in human aortic ECs (hAoECs). Shown is one representative experiment of three, performed in triplicate. Isotype control staining is shown in red. **(B)** Permeability of hAoECs to FITC-dextran after stimulation with TNFα (10 ng/ml) for 24 h. (n=14-20 wells from 6 independent experiments; Student's t-test). **(C)** Staining of β-catenin in human atherosclerotic lesions. Human carotid endarterectomy specimens were stained for β-Catenin (ABC; brown) in combination with CD31 (pink). Scale bar = 50 µm. **(D)** WNT

activity in hAoECs was measured using a Gaussia luciferase WNT reporter assay. Cells were transiently transfected with a β -catenin-activated reporter and treated with WNT3a (100 ng/ml) and the WNT inhibitor endo-IWR1 (10 μ M), as indicated. The activity of secreted Gaussia luciferase was quantified in the supernatant after 24 h. (n = 3, 2-way ANOVA with Bonferroni post-test). **(E)** Quantification of β -catenin mRNA levels in hAoECs by qPCR, normalized to *GAPDH*. Cells were treated with CXCL12 (100 ng/ml), AMD3100 (1 μ g/ml) or a combination, as indicated (n=4-5; Kruskal-Wallis test with Dunn's post-test). **(F)** Immunofluorescence analysis of β -catenin after treatment with CXCL12 (100 ng/ml) for 24 h. Scale bar = 30 μ m. **(G)** Quantification of mRNA levels of the WNT target genes *MTI*, *cyclin-D1* and *axin-2* by qPCR, normalized to *GAPDH*. Cells were treated with CXCL12 (100 ng/ml), AMD3100 (1 μ g/ml) or endo-IWR1 (10 μ M) for 3 d, as indicated (n=3; Kruskal-Wallis test with Dunn's post-test). **(H)** Permeability of hAoECs to FITC-Dextran after stimulation with CXCL12 (100 ng/ml) for 15 min. Cells were pretreated with endo-IWR1 (1 μ M) for 1 h (n=5-9 wells from 3 independent experiments; 1-way ANOVA with Tukey's post-test). **(I)** Quantification of *VE-cadherin* mRNA levels by qPCR, normalized to *GAPDH*. Cells were treated with CXCL12 (100 ng/ml) and endo-IWR1 (10 μ M), as indicated (n=3; 1-way ANOVA with Tukey's post-test). **(B-I)** Data represent mean \pm SD. * P <0.05; ** P <0.01; *** P <0.001.

Supplemental Figure 5: Effects of CXCR4 on EC and SMC mediated vascular reactivity and SMC proliferation, migration and phenotype. **(A-C)** Vascular contraction and relaxation was measured on aortic rings from *BmxCre*⁺ vs *BmxCre*⁻*Cxcr4*^{fl/fl}*Apoe*^{-/-} mice after 12 weeks of HFD or chow diet, as indicated. Data represent mean \pm SEM. **(A)** Phenylephrine-triggered vascular contraction (n=4-6 rings from 4-6 mice). **(B)** Endothelium-dependent relaxation triggered by acetylcholine, which stimulates endothelial NO production (n=14-22 rings from 6-9 mice). **(C)** Endothelium-independent relaxation triggered by the NO donor DETA-NONOate (n=14-22 rings from 6-9 mice). **(D-E)** Expression of the proliferation marker PCNA in *TaglnCre*⁺*Cxcr4*^{fl/fl}*Apoe*^{-/-} mice compared to *TaglnCre*⁻ controls after 12 weeks of high-fat diet **(D)** or chow diet **(E)**, as analyzed by western blot and densitometry quantification normalized to β -actin (n=6; Mann-Whitney test, ** P <0.01). Representative western blots are shown. Data represent mean \pm SD. **(F)** Human aortic SMCs treated with CXCL12 (100 ng/ml) or AMD3100 (1 μ g/ml) for 21 h, as indicated, were scratched and cell migration into the wounded area was quantified after 15 h. Numbers of migrated cells per mm scratch length are shown. Data present mean \pm SD, ** P <0,01 (n=9-10; 1-way ANOVA with Tukey's post-test). **(G)** Quantification of CXCR4 surface expression by flow cytometry in human aortic SMCs. Gating of cells by FSC/SSC and CXCR4 surface expression as mean fluorescence intensity, with or without CXCL12 stimulation (100 ng/ml) for 18 h. The dashed horizontal line indicates the level of the isotype control. Shown is one representative experiment performed in triplicate. Repre-

sentative histogram of CXCR4 expression (below graph). **(H/I)** Diastolic **(H)** and systolic **(I)** blood pressure in *TaglnCre⁻* and *TaglnCre⁺ Cxcr4^{fl/fl} Apoe^{-/-}* mice measured using non-invasive blood pressure tail cuffs (n=6 each). Data represent mean±SD. Statistical analysis by Student's t-test with Welch correction or Mann-Whitney test, as appropriate. **(J-L)** Vascular relaxation and contraction was measured on aortic rings from *TaglnCre⁺* vs *TaglnCre⁻ Cxcr4^{fl/fl} Apoe^{-/-}* mice on chow diet. Where indicated, the endothelium was removed from the aortic rings before measurement. **(J)** Acetylcholine-induced endothelium-dependent relaxation (n=10-12 rings from 7 mice each; mean ± SEM). **(K)** DETA-NONOate-induced endothelium-independent relaxation (n=6 rings from 6 mice each; mean ± SEM). **(L)** Ratio of L-NAME-induced contraction (300 μM L-NAME) to basal precontraction without L-NAME (n=10-11 rings from 7 mice each; mean ± SD). **(M-N)** Nitric oxide (NO) levels in plasma of *TaglnCre⁺* and *TaglnCre⁻ Cxcr4^{fl/fl} Apoe^{-/-}* mice after chow diet (**M**; n=12) and 12 weeks of HFD (**N**; HFD; n=8-9). Data represent mean±SD. Statistical analysis by Student's t-test with Welch correction or Mann-Whitney test, as appropriate. **(O-Q)** Vascular relaxation and contraction was measured on aortic rings from *SmmhcCre⁺* vs *SmmhcCre⁻ Cxcr4^{fl/fl} Apoe^{-/-}* mice on chow diet. **(O)** Acetylcholine-induced endothelium-dependent relaxation (n=12-30 rings from 3-8 mice each; mean ± SEM). **(P)** DETA-NONOate-induced endothelium-independent relaxation (n=12-30 rings from 3-8 mice each; mean ± SEM). **(Q)** Ratio of L-NAME-induced contraction (300 μM L-NAME) to basal precontraction without L-NAME (n=12-30 rings from 3-8 mice each; mean ± SD). **(J,K,O,P)** 2-way repeated measures ANOVA with Bonferroni post-test for comparison *Cre⁻* vs *Cre⁺*; **(L-N, Q)** Student's t-test with Welch correction or Mann-Whitney test, as appropriate; */**/** for *Cre⁻* vs *Cre⁺* with endothelium; §§§ for *Cre⁻* without endothelium vs *Cre⁺* without endothelium. **P*<0.05; ***P*<0.01 and ***/§§§*P*<0.001. **(R-U)** Evaluation of SMC phenotype by gene expression analysis. **(R-S)** Relative quantification of *Tagln*, *Smmhc*, *vimentin* and *CD248* (endosialin) mRNA expression in thoracic aortas of **(R)** *TaglnCre⁺* vs *TaglnCre⁻ Cxcr4^{fl/fl} Apoe^{-/-}* and **(S)** *SmmhcCre⁺* vs *SmmhcCre⁻ Cxcr4^{fl/fl} Apoe^{-/-}* mice on normal chow diet, after normalization to *18S* rRNA (n = 5-9). **(T)** Relative quantification of *CNN1* mRNA expression in hAoSMCs, pretreated with endoIWR1 (1 μM) and stimulated with WNT3a (200 ng/ml), as indicated. Data are normalized to *GAPDH* expression (data from 5 experiments). **(U)** Relative quantification of *CNN1* mRNA in hAoSMCs stimulated with (protease-resistant) CXCL12 (100-300 ng/ml), TGF-β (2.5 ng/ml) or PDGF-BB (20 ng/ml) as indicated. Data are normalized to *GAPDH* expression (data from 5-6 experiments, each performed in triplicate). **(R-U)** Data represent mean±SD, **P*<0.05; ***P*<0.01 and ****P*<0.001 by t-test with Holm-Sidak's post-test as a correction for multiple testing **(R,S)** or one-way ANOVA with Sidak's post-test or Kruskal-Wallis test with Dunn's post-test **(T,U)**, as appropriate.

Supplemental References

1. Nie Y, Waite J, Brewer F, Sunshine MJ, Littman DR, Zou YR. The role of CXCR4 in maintaining peripheral B cell compartments and humoral immunity. *J Exp Med*. 2004;200:1145-1156.
2. Ehling M, Adams S, Benedito R, Adams RH. Notch controls retinal blood vessel maturation and quiescence. *Development*. 2013;140:3051-3061.
3. Holtwick R, Gotthardt M, Skryabin B, Steinmetz M, Potthast R, Zetsche B, Hammer RE, Herz J, Kuhn M. Smooth muscle-selective deletion of guanylyl cyclase-A prevents the acute but not chronic effects of ANP on blood pressure. *Proc Natl Acad Sci U S A*. 2002;99:7142-7147.
4. Wirth A, Benyo Z, Lukasova M, Leutgeb B, Wettschureck N, Gorbey S, Orsy P, Horvath B, Maser-Gluth C, Greiner E, Lemmer B, Schutz G, Gutkind JS, Offermanns S. G12-G13-LARG-mediated signaling in vascular smooth muscle is required for salt-induced hypertension. *Nat Med*. 2008;14:64-68.
5. Broermann A, Winderlich M, Block H, Frye M, Rossaint J, Zarbock A, Cagna G, Linnepe R, Schulte D, Nottebaum AF, Vestweber D. Dissociation of VE-PTP from VE-cadherin is required for leukocyte extravasation and for VEGF-induced vascular permeability in vivo. *J Exp Med*. 2011;208:2393-2401.
6. Döring Y, Soehnlein O, Drechsler M, Shagdarsuren E, Chaudhari SM, Meiler S, Hartwig H, Hristov M, Koenen RR, Hieronymus T, Zenke M, Weber C, Zernecke A. Hematopoietic interferon regulatory factor 8-deficiency accelerates atherosclerosis in mice. *Arterioscler Thromb Vasc Biol*. 2012;32:1613-1623.
7. Strehlow K, Werner N, Berweiler J, Link A, Dirnagl U, Priller J, Laufs K, Ghaeni L, Milosevic M, Böhm M, Nickenig G. Estrogen increases bone marrow-derived endothelial progenitor cell production and diminishes neointima formation. *Circulation*. 2003;107:3059-3065.
8. Cho HJ, Kim HS, Lee MM, Kim DH, Yang HJ, Hur J, Hwang KK, Oh S, Choi YJ, Chae IH, Oh BH, Choi YS, Walsh K, Park YB. Mobilized endothelial progenitor cells by granulocyte-macrophage colony-stimulating factor accelerate reendothelialization and reduce vascular inflammation after intravascular radiation. *Circulation*. 2003;108:2918-2925.
9. Rennert RC, Sorkin M, Garg RK, Gurtner GC. Stem cell recruitment after injury: lessons for regenerative medicine. *Regen Med*. 2012;7:833-50.
10. Reynolds JL, Joannides AJ, Skepper JN, McNair R, Schurgers LJ, Proudfoot D, Jahnen-Dechent W, Weissberg PL, Shanahan CM. Human vascular smooth muscle cells undergo vesicle-mediated calcification in response to changes in extracellular calcium and phosphate concentrations: a potential mechanism for accelerated vascular calcification in ESRD. *J Am Soc Nephrol*. 2004;15:2857-67.
11. Segers VF, Tokunou T, Higgins LJ, MacGillivray C, Gannon J, Lee RT. Local delivery of protease-resistant stromal cell derived factor-1 for stem cell recruitment after myocardial infarction. *Circulation*. 2007;116:1683-1692.
12. Projahn D, Simsekylmaz S, Singh S, Kanzler I, Kramp BK, Langer M, Burlacu A, Bernhagen J, Klee D, Zernecke A, Hackeng TM, Groll J, Weber C, Liehn EA, Koenen RR. Controlled intramyocardial release of engineered chemokines by biodegradable hydrogels as a treatment approach of myocardial infarction. *J Cell Mol Med*. 2014;18:790-800.
13. Egea V, Zahler S, Rieth N, Neth P, Popp T, Kehe K, Jochum M, Ries C. Tissue inhibitor of metalloproteinase-1 (TIMP-1) regulates mesenchymal stem cells through let-7f microRNA and Wnt/beta-catenin signaling. *Proc Natl Acad Sci U S A*. 2012;109:E309-316.

14. Asztalos BF, de la Llera-Moya M, Dallal GE, Horvath KV, Schaefer EJ, Rothblat GH. Differential effects of HDL subpopulations on cellular ABCA1- and SR-BI-mediated cholesterol efflux. *J Lipid Res.* 2005;46:2246-2253.
15. Golbus JR, Stitzel NO, Zhao W, Xue C, Farrall M, McPherson R, Erdmann J, Deloukas P, Watkins H, Schunkert H, Samani NJ, Saleheen D, Kathiresan S, Reilly MP. Common and Rare Genetic Variation in CCR2, CCR5, or CX3CR1 and Risk of Atherosclerotic Coronary Heart Disease and Glucometabolic Traits. *Circ Cardiovasc Genet.* 2016;9:250-258.
16. Borenstein M, Hedges LV, Higgins JPT, Rothstein HR (2009) Introduction to meta-analysis. Chichester, UK: Wiley.
17. Holdt LM, Beutner F, Scholz M, Gielen S, Gabel G, Bergert H, Schuler G, Thiery J, Teupser D. ANRIL expression is associated with atherosclerosis risk at chromosome 9p21. *Arteriosclerosis, thrombosis, and vascular biology.* 2010;30:620-7.
18. Holdt LM, Stahring A, Sass K, Pichler G, Kulak NA, Wilfert W, Kohlmaier A, Herbst A, Northoff BH, Nicolaou A, Gabel G, Beutner F, Scholz M, Thiery J, Musunuru K, Krohn K, Mann M, Teupser D. Circular non-coding RNA ANRIL modulates ribosomal RNA maturation and atherosclerosis in humans. *Nat Commun.* 2016;7:12429.
19. El Housni H, Heimann P, Parma J, Vassart G. Single-nucleotide polymorphism genotyping by melting analysis of dual-labeled probes: Examples using factor v leiden and prothrombin 20210a mutations. *Clin Chem.* 2003;49:1669-1672.